FEBS Letters 583 (2009) 3204–3208

FEBS Letters

journal homepage: www.FEBSLetters.org

Large-scale movement of functional domains facilitates aminoacylation by human mitochondrial phenylalanyl-tRNA synthetase

Srujana S. Yadavalli [a], Liron Klipcan [c], Alexey Zozulya [d], Rajat Banerjee [a], Dmitri Svergun [d], Mark Safro [c,*], Michael Ibba [a,b,*]

[a] Department of Microbiology and Center for RNA Biology, Ohio State University, Columbus, OH 43210, USA
[b] Ohio State Biochemistry Program, Ohio State University, Columbus, OH 43210, USA
[c] Department of Structural Biology, Weizmann Institute of Science, 76100 Rehovot, Israel
[d] EMBL, Hamburg Outstation, Notkestrasse 85, 22603 Hamburg, Germany

ARTICLE INFO

Article history:
Received 24 August 2009
Revised 31 August 2009
Accepted 1 September 2009
Available online 6 September 2009

Edited by Hans Eklund

Keywords:
Aminoacylation
Mitochondrion
Protein synthesis
tRNA
Translation

ABSTRACT

Structural studies suggest rearrangement of the RNA-binding and catalytic domains of human mitochondrial PheRS (mtPheRS) is required for aminoacylation. Crosslinking the catalytic and RNA-binding domains resulted in a "closed" form of mtPheRS that still catalyzed ATP-dependent Phe activation, but was no longer able to transfer Phe to tRNA and complete the aminoacylation reaction. SAXS experiments indicated the presence of both the closed and open forms of mtPheRS in solution. Together, these results indicate that conformational flexibility of the two functional modules in mtPheRS is essential for its phenylalanylation activity. This is consistent with the evolution of the aminoacyl-tRNA synthetases as modular enzymes consisting of separate domains that display independent activities.

1. Introduction

Aminoacyl-tRNA synthetases (aaRSs) play a key role in maintaining translational fidelity by synthesizing correctly paired aminoacyl-tRNAs (aa-tRNAs) [1,2]. Aminoacyl-tRNA synthesis occurs in two steps: (i) amino acid activation forming aminoacyl-adenylate (aa-AMP) and (ii) transfer of amino acid to the 3′ end of cognate tRNA. While some aaRSs are highly selective for their substrate amino acids, others require a correction mechanism called "editing" to eliminate the incorrect products [3,4]. AaRSs are divided into two mutually exclusive groups, class I and class II, based on their structure and function [5–7]. Class I aaRSs are usually monomeric, whereas class II aaRSs mostly function as dimers or tetramers. A common feature of all aaRS enzymes is the modular arrangement of functional units along the sequence [8]. For example, in class I and class IIc aaRSs the N-terminal half is a catalytic domain responsible for aa-AMP synthesis, and RNA recognition elements are present in the C-terminal region. It is believed that the catalytic domain constitutes the ancestral core enzyme to which several accessory domains including sequences important for RNA recognition, oligomerization, assembly and complex formation have been appended later in evolution [9].

Phenylalanyl-tRNA synthetase (PheRS), a class IIc aaRS, exists as an $(\alpha\beta)_2$ heterotetramer in the bacterial [10] and eukaryal cytosolic forms [11], where the α subunit constitutes the catalytic module and the B3/B4 domain of the β subunit forms the editing site [12,13]. PheRS is instead active as a monomer in the organelles of eukaryotes [14,15] and lacks an editing function [16]. Human mitochondrial PheRS (mtPheRS) is highly homologous to the corresponding domains of bacterial PheRS, consisting of an N-terminal catalytic α domain fused to a C-terminal B8-like anticodon-binding domain (ABD) from the β subunit [17]. The crystal structure of mtPheRS revealed a fully closed conformation in which the anticodon-binding domain, located at the C-terminus, overlaps with the acceptor stem of $tRNA^{Phe}$ when the substrate is modeled in a position similar to that seen in the bacterial heterotetrameric PheRS–$tRNA^{Phe}$ complex (see [17] for a complete docking model). To bind $tRNA^{Phe}$ correctly, the ABD must undergo a ~160° hinge-type rotation upon tRNA binding [17]. MtPheRS is therefore proposed to exist in two conformations: a "closed" state when it

Abbreviations: aaRS, aminoacyl-tRNA synthetase; mtPheRS, mitochondrial phenylalanyl-tRNA synthetase; ABD, anticodon-binding domain

* Corresponding authors. Address: Department of Microbiology and Center for RNA Biology, Ohio State University, Columbus, OH 43210, USA. Fax: +1 614 292 8120 (M. Ibba), +972 8 934 41 36 (M. Safro).
E-mail addresses: mark.safro@weizmann.ac.il (M. Safro), ibba.1@osu.edu (M. Ibba).

0014-5793/$36.00
doi:10.1016/j.febslet.2009.09.008

is not bound to the tRNA and an "open" state upon tRNA binding. To test this hypothesis, we restrained the movement of the ABD relative to the catalytic domain, which led to a loss in aminoacylation but not Phe activation. SAXS analysis confirmed the existence of the open and closed states in solution, underscoring the importance of conformational mobility in mtPheRS for maintaining the function of this essential housekeeping enzyme.

2. Materials and methods

2.1. Protein expression, purification and characterization

Escherichia coli strain BL21 (pArgU218)/pET21c-PheRS expressing C-terminal His6-tagged mtPheRS was a gift from Dr. L. Spremulli (University of North Carolina, Chapel Hill, NC). Primers were obtained from IDT (Integrated DNA Technologies). Rosetta (DE3) cells containing pRARE plasmids encoding tRNAs for rare codons were transformed with the mutant mtPheRS plasmid construct and selected on medium containing both ampicillin and chloramphenicol. The cells were grown at 37 °C to OD = 0.8 and induced with 0.5 mM IPTG for 4 h. Cells were harvested, sonicated and supernatant was collected after centrifugation at 25 000×*g* for 1 h. The supernatant was applied to a TALON® metal affinity resin column (Clontech), followed by washing and the protein was eluted with 25 mM Tris–HCl, pH 8.0, 300 mM NaCl, 250 mM imidazole and 10% glycerol. Fractions containing mtPheRS were checked for electrophoretic purity by SDS–PAGE, pooled and dialyzed overnight at 4 °C in 50 mM Tris–HCl, pH 7.5, 5 mM $MgCl_2$ and 100 mM KCl. The purified enzyme was concentrated, adjusted to 50% (v/v) glycerol and aliquots were stored at −80 °C. The presence of disulfide bonds in K33C/T351C mtPheRS was determined by non-reducing SDS–PAGE. Samples were mixed with a loading buffer containing 100 mM Tris–HCl, pH 6.8, 10% (v/v) glycerol, 2% (w/v) SDS, 0.05% (w/v) bromophenol blue and 10 mM DTT (for reduced samples only) before electrophoresis. The proteins were resolved with a 4–15% pre-cast polyacrylamide gel (Bio-Rad) and visualized using coomassie blue staining. Aminoacylation and active site titration assays were performed as previously described [18,19].

2.2. Fluorescence intensity measurements and tRNA binding

2AP-labeled *E. coli* $tRNA^{Phe}$ was synthesized as described previously [20]. Different concentrations of WT and mutant mtPheRS were allowed to equilibrate with 0.1 μM 2AP-$tRNA^{Phe}$ in 0.1 M Tris, pH 7.5, for 15 min. Fluorescence intensities of protein–tRNA complexes were measured using a Fluorolog-3 spectrafluorimeter (Horiba Jobin Yvon). From the fluorescence intensity curves, area under the curve (AUC) was determined. The percentage increase in AUC with increase in protein concentration was then compared.

2.3. Small angle X-ray scattering (SAXS)

Synchrotron small angle X-ray scattering data were collected at the bending magnet beamline X33 (DORIS III storage ring, DESY) of the EMBL Hamburg Outstation using a pixel detector PILATUS 1 M (DECTRIS, Switzerland). To monitor for radiation damage, four successive 30 s exposures of the same sample were done and no changes were detected. The sample-to-detector distance was 2.7 m providing the range of scattering vectors $0.08 < s < 6\ nm^{-1}$ ($s = 4\pi\sin\theta/\lambda$, where 2θ is the scattering angle and $\lambda = 0.15$ nm is the X-ray wavelength). Solutions of mtPheRS alone and its complex with tRNA were measured at three different concentrations of mtPheRS in the range from 1 to 5 mg/ml (sample temperature 10 °C). The data were processed following standard procedures using PRIMUS [21] and GNOM [22], and calibrated against a reference solution of bovine serum albumin (MM = 66 kDa) to determine the overall parameters (molecular mass, radius of gyration R_g, and maximal diameter D_{max}). The estimation of excluded volume V_{ex} and low-resolution ab initio models of mtPheRS solutes were obtained using DAMMIF [23,24]. This program builds a compact interconnected bead model fitting the experimental data $I_{exp}(s)$ to minimize discrepancy:

$$\chi^2 = \frac{1}{N-1}\sum_j \left[\frac{I_{exp}(s_j) - cI_{calc}(s_j)}{\sigma(s_j)}\right]^2,$$

where N is the number of experimental points, c is a scaling factor and $I_{calc}(s)$ and $\sigma(sj)$ are the calculated intensity and the experimental error at the momentum transfer sj, respectively. The scattering patterns from the atomic models were computed by CRYSOL [25]. The volume fractions of mtPheRS–tRNA complex and free tRNA as well as fitting to the measured SAXS data were computed using OLIGOMER [21].

3. Results

3.1. Catalytic activity of open and closed mtPheRS

Residues K33 and T351 of mtPheRS are separated by ~5 Å, and were both replaced by cysteines to allow disulfide bond formation and subsequent crosslinking of the enzyme in a closed form. Wild-type (WT) and K33C/T351C mtPheRS samples were subjected to electrophoresis under reducing and non-reducing conditions (Fig. 1). Both the samples migrated to a similar extent when 10 mM DTT (reducing conditions) was included in the sample loading buffer (lanes 1 and 2; monomeric mtPheRS, ~48 kDa) while K33C/T351C mtPheRS migrated differently (lane 4) compared to WT (lane 3) under non-reducing conditions. The faster migration of the mutant is consistent with the formation of an intramolecular disulfide bond between the two cysteines at positions 33 and 351. In addition, intermolecular disulfide bond formation was observed in both the WT as well as double cysteine mutant mtPheRSs, forming dimers of ~96 kDa. This is expected considering the presence of six cysteines in WT mtPheRS. None of these six cysteines are in proximity to each other or to the newly introduced cysteine residues at positions 33 and 351, ruling out the possibility of the formation of other intramolecular disulfide bonds. Additionally, titration of the free thiols using Ellman's reagent, 5,5′-dithiobis-2-nitrobenzoic acid (DTNB) or 4,4′-dithiopyridine (DTDP) confirmed the presence of equal numbers of reactive thiol groups in

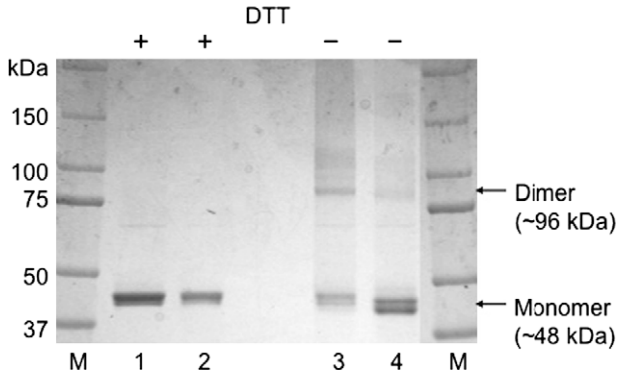

Fig. 1. SDS–PAGE analysis of purified human mtPheRS. WT and mutant mtPheRS samples were analyzed on a 4–15% (w/v) polyacrylamide gradient gel and the proteins were visualized by staining with Coomassie blue. Lanes 1 and 2 show WT and K33C/T351C mtPheRSs, respectively, in the presence of 10 mM DTT. Lanes 3 and 4 represent WT and K33C/T351C mtPheRSs under non-reducing conditions. M stands for molecular weight marker.

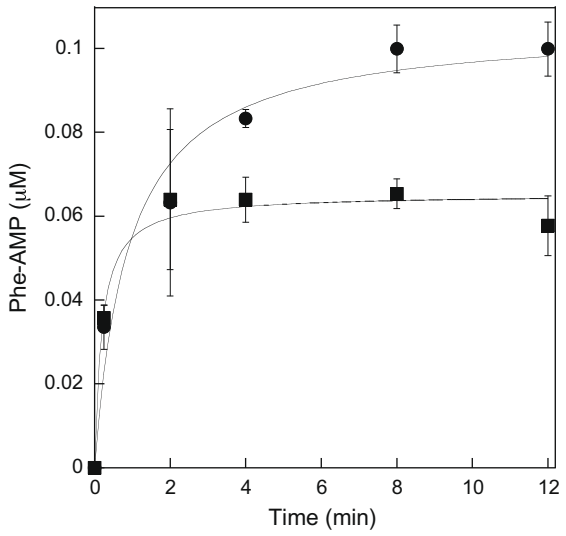

Fig. 2. Formation of PheRS:Phe-AMP complex. Phenylalanyl–adenylate complex formation by WT (●) and K33C/T351C (■) mtPheRSs.

the WT and mutant mtPheRSs under non-reducing conditions (data not shown).

WT and mutant mtPheRSs were tested for their ability to catalyze the first step in aminoacylation, the formation of enzyme-bound aa-AMP, in the absence of reducing agents. Time courses for PheRS-Phe-AMP formation were monitored using the active site titration protocol. The closed form of the K33C/T351C mutant was able to form stable enzyme Phe-AMP complexes at approximately 60% of the level shown by WT mtPheRS under the same conditions (Fig. 2). These data indicate that the first step of the Phe-tRNA synthesis pathway, Phe-AMP formation, is not dependent on the conformational state of mtPheRS. Next we investigated the ability of open and closed mtPheRS to catalyze the second step of the aminoacylation reaction by monitoring Phe-tRNA accumulation. Aminoacylation assays performed under non-reducing conditions suggest that K33C/T351C mtPheRS has negligible activity compared to WT when it is restrained in the closed conformation (Fig. 3A). Addition of 10 mM DTT to the aminoacylation reaction, which allows K33C/T351C mtPheRS to adopt an open conformation, increased Phe-tRNA synthesis by the mutant to approximately 90% of WT level (Fig. 3B), indicating that conformational flexibility of functional domains is essential for the aminoacylation activity of mtPheRS.

3.2. tRNA binding by mtPheRS

It is possible that either the closed form of K33C/T351C mtPheRS is unable to bind $tRNA^{Phe}$ or that binding does not result in the correct conformational change necessary for $tRNA^{Phe}$ aminoacylation. In order to test these two possibilities, we attempted to measure binding constants for $tRNA^{Phe}$ using fluorescence techniques. It has been estimated previously that mtPheRS has a K_m for $tRNA^{Phe}$ of ~18 μM [15] which, given the low yields of active mitochondrial $tRNA^{Phe}$ transcribed in vitro, precludes accurate determination of binding constants. Comparison of binding at sub-saturating non-reducing concentrations suggests that WT mtPheRS binds $tRNA^{Phe}$ better than the closed mutant form (Fig. 3C), consistent with the proposal that conformational flexibility is crucial for maintaining the aminoacylation function. The conformational flexibility in solution of mtPheRS was further investigated by small angle X-ray scattering (SAXS).

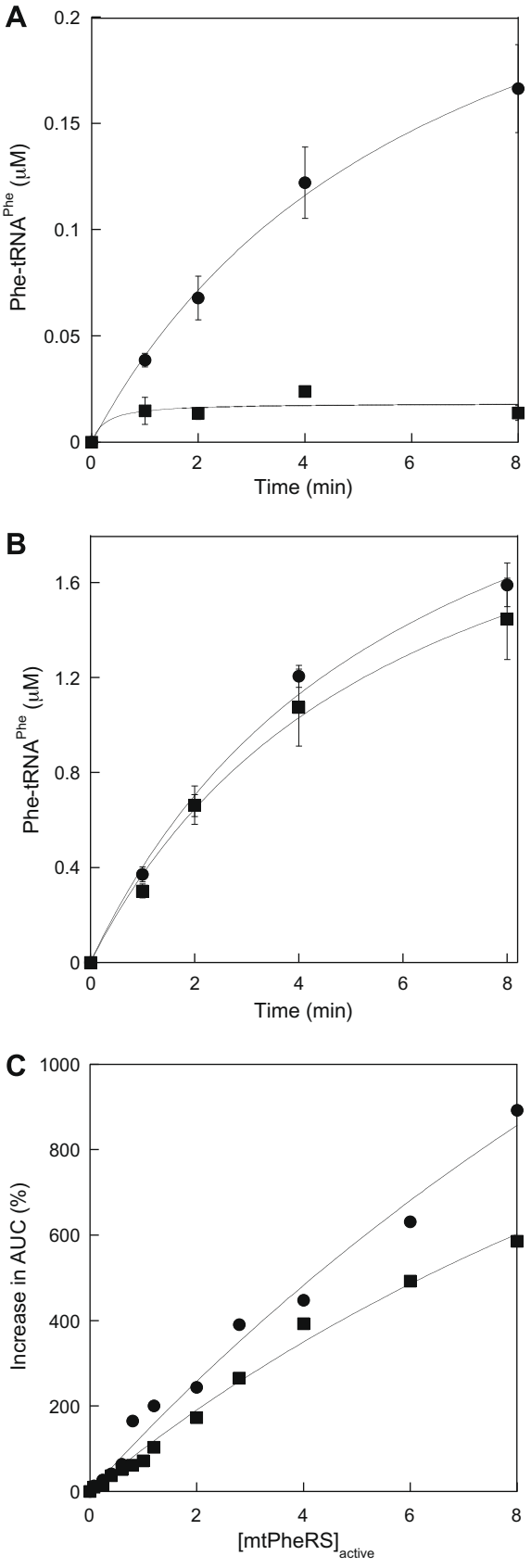

Fig. 3. $tRNA^{Phe}$ binding and aminoacylation. Phenylalanylation by mtPheRSs (0.4 μM) in the absence of any reducing agents (A), and in the presence of 10 mM DTT (B). (C) binding of $tRNA^{Phe}$ to mtPheRS. WT (●) and K33C/T351C (■) mtPheRS under non-reducing conditions.

Table 1
Overall structural parameters evaluated from SAXS data.

Sample	R_g, nm	MM_{exp}, kDa	MM_{calc}, kDa	D_{max}, nm	V_{ex}, nm^3	χ
MtPheps	3.03	46.4	48.4	10.5	98	1.38
MtPheRs + tRNA	3.12	68.7	71	12.5	80	1.60
Ratio	1.03	1.48	1.47	1.2	0.82	–

R_g, MM_{exp}, D_{max} and V_{ex} are the radius of gyration, molecular mass (MM), maximum size, and excluded volume derived from scattering data. MM_{calc} is the MM calculated from primary sequence. χ values are the discrepancies between experimental data and calculated scattering curves.

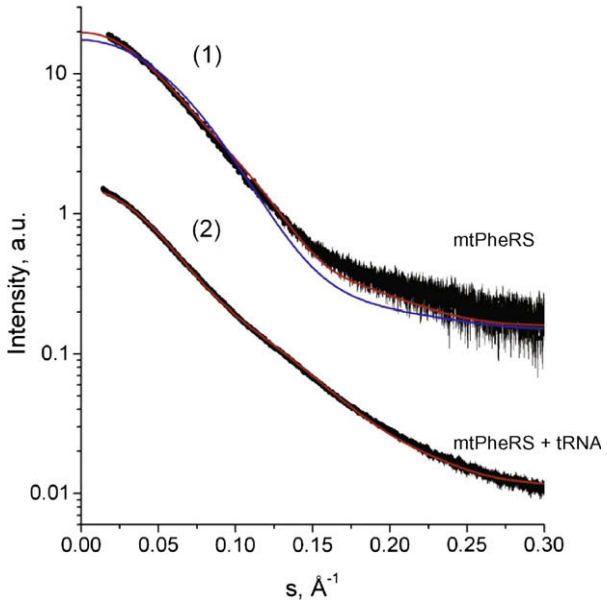

Fig. 4. Scattering profiles of mtPheRS alone and its complex with tRNA. Experimental SAXS data of mtPheRS alone (curve 1) and the complex (curve 2) are represented in logarithmic scale by dots with error bars. The fitting curves are shown by solid lines. Fits obtained from the crystal structures of "closed" and "opened" conformations of mtPheRS are shown in (1) as blue and red lines, respectively. Fit obtained by OLIGOMER for the model of the complex is shown in (2) as red line. For better visualization the scattering curve of the protein was multiplied by a factor of 20.

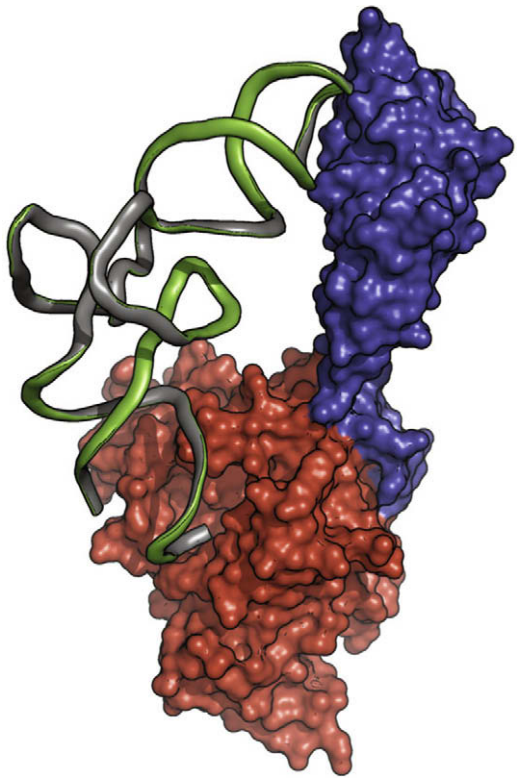

Fig. 5. Rigid body model of mtPheRS in complex with tRNA. MtPheRS is colored red, anticodon-binding domain of mtPheRS is colored blue and tRNA is shown in green.

3.3. Modeling of mtPheRS structure by SAXS

The conformations of mtPheRS both alone and in complex with tRNA were probed by SAXS. The overall parameters of mtPheRS and the mtPheRS-tRNA^{Phe} complex are summarized in Table 1. The experimental scattering curve from native mitPheRS (Fig. 4, curve 1, scatter) cannot be adequately fitted by the calculated scattering curve from the crystal structure of mtPheRS (PDB code 3cmq.pdb, [17]) showing the discrepancy $\chi = 3.04$ (Fig. 4, curve 1, blue line). At the same time, the fit calculated from the proposed open conformation of mtPheRS [17] provides much better agreement with the experimental data with the discrepancy $\chi = 1.38$ (Fig. 4, curve 1, red line). However, smearing of the scattering profile suggests that the structure in solution may be flexible. Such a conformational mobility would not be surprising due to the extended linker region (residues 290–322 in mature mtPheRS), connecting the catalytic module of the enzyme to the anticodon-binding domain. These results are indicative of the conformational flexibility of mtPheRS that exists in solution, and demonstrate that both the "crystal" and "solution forms" are two functionally relevant states.

Given that the solution of the complex contained excess tRNA, no direct modeling of its structure was possible. A set of tentative models of the complex, which obey the contact conditions, was generated interactively by MASSHA [26]. The scattering patterns of these models were calculated and taken in a linear combination with the computed scattering from the tRNA molecule (PDB code 1eiy) to fit the experimental pattern from the complex using OLIGOMER. The overall best model (Fig. 5) provides the fit with $\chi = 1.60$ (Fig. 4, curve 2) at the volume fractions of 53% and 47% for the 1:1 mtPheRS–tRNA complex and free tRNA, respectively. This model further suggests that the formation of the mtPheRS–tRNA complex is accompanied by significant rearrangement of the anticodon-binding domain.

4. Discussion

4.1. The open conformation of mtPheRS aminoacylates tRNA^{Phe}

Biochemical data indicate that while the open form of mtPheRS only binds tRNA^{Phe} moderately more strongly than the closed form, only the open form is competent in aminoacylation. This is consistent with models of the open form derived from the crystal structure of mtPheRS, which suggested that accurate binding of tRNA recognition elements would necessitate a large conformational rearrangement in the C-terminal anticodon-binding domain. The use of SAXS to augment existing crystallographic data confirmed the existence of the open form of mtPheRS, and provided a model for tRNA^{Phe} recognition. As seen for other class II aaRSs, mtPheRS

recognizes the major groove side of the acceptor stem (Fig. 5) but does so via an unusually small contact region with $tRNA^{Phe}$ (74 and 17 protein residues for bacterial and mitochondrial PheRSs, respectively). The majority of the interactions with $tRNA^{Phe}$ are concentrated around the anticodon loop and 3′-CCA-end, and the corresponding amino acid sequences are strictly conserved throughout bacterial and mitochondrial PheRSs and also occupy similar positions in space. These data indicate that mtPheRS has only retained the common, evolutionarily conserved, $tRNA^{Phe}$ recognition domains while losing idiosyncratic structures such as the B2 RNA-binding domain of bacterial PheRS [27]. This minimal recognition strategy is consistent with the ability of monomeric mtPheRS to efficiently cross-aminoacylate $tRNA^{Phe}$ from *E. coli*, *Thermus thermophilus* and yeast cytoplasm, a property absent from $(\alpha\beta)_2$-type PheRSs (M.S., M.I., unpublished data).

4.2. Evolution of mtPheRS and the modularity of aaRSs

The protein–RNA recognition interface of mtPheRS is considerably smaller than that of its cytoplasmic counterparts, reflecting the loss of several accessory domains during evolution of the organellar enzyme from its bacterial ancestor [16,28]. This reduction in the size and complexity of organellar PheRS explains both the relaxed specificity of $tRNA^{Phe}$ recognition (above) and the reliance on a large conformational change to complete aminoacylation. $(\alpha\beta)_2$-type PheRSs bind tRNA across more than one subunit [10], while the monomeric mtPheRS instead ensures accurate recognition and aminoacylation by co-ordinating the movement of the N- and C-terminal domains, which bind the 3′-CCA and anticodon of tRNA, respectively. These data reveal how conserved modules can maintain the canonical role of PheRS, Phe-$tRNA^{Phe}$ synthesis, in different structural contexts despite the presence or absence of idiosyncratic modules with roles ranging from proofreading to DNA-binding [16,29]. AaRSs are believed to have evolved in a piece-wise fashion where different modules are arranged along the protein sequence [8]. Our data now show that the functional independence of such modules ensures canonical aaRS activity is retained despite the frequent addition or loss of other secondary activities during evolution. This structural and evolutionary versatility allows aaRSs to acquire functions outside protein synthesis, where they have recently been shown to play numerous key roles [30,31].

Acknowledgements

We thank H. Roy and T. Rogers for critical reading of the manuscript. This work was supported by grants from the Binational Science Foundation (2005209, MS and MI), National Science Foundation (744791, MI), and the EU Design Study SAXIER (011934, AVZ and DIS). LK is grateful to the Ori Foundation for a doctoral research fellowship.

References

[1] Ataide, S.F. and Ibba, M. (2006) Small molecules – big players in the evolution of protein synthesis. ACS Chem. Biol. 1, 285–297.
[2] Ling, J., Reynolds, N. and Ibba, M. (2009) Aminoacyl-tRNA synthesis and translational quality control. Annu. Rev. Microbiol. 63, 61–78.
[3] Jakubowski, H. and Goldman, E. (1992) Editing of errors in selection of amino acids for protein synthesis. Microbiol. Rev. 56, 412–429.
[4] Hendrickson, T.L. and Schimmel, P. (2003) Transfer RNA-dependent amino acid discrimination by aminoacyl-tRNA synthetases in: Translation Mechanisms (Lapointe, J. and Brakier-Gingras, L., Eds.), pp. 34–64, Kluwer Academic/Plenum Publishers.
[5] Cusack, S., Berthet-Colominas, C., Hartlein, M., Nassar, N. and Leberman, R. (1990) A second class of synthetase structure revealed by X-ray analysis of *Escherichia coli* seryl-tRNA synthetase at 2.5 Å. Nature 347, 249–255.
[6] Eriani, G., Delarue, M., Poch, O., Gangloff, J. and Moras, D. (1990) Partition of tRNA synthetases into two classes based on mutually exclusive sets of sequence motifs. Nature 347, 203–206.
[7] Ribas De Pouplana, L. and Schimmel, P. (2001) Two classes of tRNA synthetases suggested by sterically compatible dockings on tRNA acceptor stem. Cell 104, 191–193.
[8] Alexander, R.W. and Schimmel, P. (2001) Domain–domain communication in aminoacyl-tRNA synthetases. Prog. Nucleic Acid Res. Mol. Biol. 69, 317–349.
[9] Ibba, M., Curnow, A.W. and Sòll, D. (1997) Aminoacyl-tRNA synthesis: divergent routes to a common goal. Trends Biochem. Sci. 22, 39–42.
[10] Goldgur, Y., Mosyak, L., Reshetnikova, L., Ankilova, V., Lavrik, O., Khodyreva, S. and Safro, M. (1997) The crystal structure of phenylalanyl-tRNA synthetase from *Thermus thermophilus* complexed with cognate tRNA Phe. Structure 5, 59–68.
[11] Moor, N., Linshiz, G. and Safro, M. (2002) Cloning and expression of human phenylalanyl-tRNA synthetase in *Escherichia coli*: comparative study of purified recombinant enzymes. Protein Expr. Purif. 24, 260–267.
[12] Roy, H., Ling, J., Irnov, M. and Ibba, M. (2004) Post-transfer editing in vitro and in vivo by the beta subunit of phenylalanyl-tRNA synthetase. EMBO J. 23, 4639–4648.
[13] Kotik-Kogan, O., Moor, N., Tworowski, D. and Safro, M. (2005) Structural basis for discrimination of L-phenylalanine from L-tyrosine by phenylalanyl-tRNA synthetase. Structure 13, 1799–1807.
[14] Sanni, A., Walter, P., Boulanger, Y., Ebel, J.P. and Fasiolo, F. (1991) Evolution of aminoacyl-tRNA synthetase quaternary structure and activity: *Saccharomyces cerevisiae* mitochondrial phenylalanyl-tRNA synthetase. Proc. Natl. Acad. Sci. USA 88, 8387–8391.
[15] Bullard, J.M., Cai, Y.C., Demeler, B. and Spremulli, L.L. (1999) Expression and characterization of a human mitochondrial phenylalanyl-tRNA synthetase. J. Mol. Biol. 288, 567–577.
[16] Roy, H., Ling, J., Alfonzo, J. and Ibba, M. (2005) Loss of editing activity during the evolution of mitochondrial phenylalanyl-tRNA synthetase. J. Biol. Chem. 280, 38186–38192.
[17] Klipcan, L., Levin, I., Kessler, N., Moor, N., Finarov, I. and Safro, M. (2008) The tRNA-induced conformational activation of human mitochondrial phenylalanyl-tRNA synthetase. Structure 16, 1095–1104.
[18] Ibba, M., Kast, P. and Hennecke, H. (1994) Substrate specificity is determined by amino acid binding pocket size in *Escherichia coli* phenylalanyl-tRNA synthetase. Biochemistry 33, 7107–7112.
[19] Ling, J., Roy, H., Qin, D., Rubio, M.A., Alfonzo, J.D., Fredrick, K. and Ibba, M. (2007) Pathogenic mechanism of a human mitochondrial tRNAPhe mutation associated with myoclonic epilepsy with ragged red fibers syndrome. Proc. Natl. Acad. Sci. USA 104, 15299–15304.
[20] Ling, J., So, B.R., Yadavalli, S.S., Roy, H., Shoji, S., Fredrick, K., Musier-Forsyth, K. and Ibba, M. (2009) Resampling and editing of mischarged tRNA prior to translation elongation. Mol. Cell 33, 654–660.
[21] Konarev, P.V., Volkov, V.V., Sokolova, A.V., Koch, M.H.J. and Svergun, D.I. (2003) PRIMUS: a windows PC-based system for small-angle scattering data analysis. J. Appl. Crystallogr. 36, 1277–1282.
[22] Svergun, D.I. (1992) Determination of regularization parameter in indirect-transform methods using perceptual criteria. J. Appl. Crystallogr. 25, 495–503.
[23] Svergun, D.I. (1999) Restoring low resolution structure of biological macromolecules from solution scattering using simulated annealing. Biophys. J. 76, 2879–2886.
[24] Franke, D. and Svergun, D.I. (2009) DAMMIF, a program for rapid ab-initio shape determination in small-angle scattering. J. Appl. Crystallogr. 42, 342–346.
[25] Svergun, D.I., Barberato, C. and Koch, M.H.J. (1995) CRYSOL – a program to evaluate X-ray solution scattering of biological macromolecules from atomic coordinates. J. Appl. Crystallogr. 28, 768–773.
[26] Konarev, P.V., Petoukhov, M.V. and Svergun, D.I. (2001) MASSHA – a graphics system for rigid-body modelling of macromolecular complexes against solution scattering data. J. Appl. Crystallogr. 34, 527–532.
[27] Roy, H. and Ibba, M. (2006) Phenylalanyl-tRNA synthetase contains a dispensable RNA binding domain that contributes to editing of non-cognate aminoacyl-tRNA. Biochemistry 45, 9156–9162.
[28] Brown, J.R. (2001) Genomic and phylogenetic perspectives on the evolution of prokaryotes. Syst. Biol. 50, 497–512.
[29] Dou, X., Limmer, S. and Kreutzer, R. (2001) DNA-binding of phenylalanyl-tRNA synthetase is accompanied by loop formation of the double-stranded DNA. J. Mol. Biol. 305, 451–458.
[30] Park, S.G., Ewalt, K.L. and Kim, S. (2005) Functional expansion of aminoacyl-tRNA synthetases and their interacting factors: new perspectives on housekeepers. Trends Biochem. Sci. 30, 569–574.
[31] Ray, P.S., Arif, A. and Fox, P.L. (2007) Macromolecular complexes as depots for releasable regulatory proteins. Trends Biochem. Sci. 32, 158–164.